Open access • Journal Article • DOI:10.1017/S0022112097008410

A universal time scale for vortex ring formation

Morteza Gharib, Edmond Rambod, Karim Shariff

Institutions: California Institute of Technology, Ames Research Center

Published on: 10 Apr 1998 - Journal of Fluid Mechanics (Cambridge University Press)

Topics: Vortex ring, Vorticity and Particle image velocimetry

J. Fluid Mech. (1998), *vol.* 360, *pp.* 121–140. Printed in the United Kingdom

A universal time scale for vortex ring formation

By MORTEZA GHARIB[1], EDMOND RAMBOD[1] AND KARIM SHARIFF[2]

[1]Graduate Aeronautical Laboratories, California Institute of Technology, Pasadena, CA 91125, USA

[2]NASA Ames Research Center, Moffett Field, CA 94035, USA

(Received 20 December 1996 and in revised form 10 November 1997)

The formation of vortex rings generated through impulsively started jets is studied experimentally. Utilizing a piston/cylinder arrangement in a water tank, the velocity and vorticity fields of vortex rings are obtained using digital particle image velocimetry (DPIV) for a wide range of piston stroke to diameter (L/D) ratios. The results indicate that the flow field generated by large L/D consists of a leading vortex ring followed by a trailing jet. The vorticity field of the leading vortex ring formed is disconnected from that of the trailing jet. On the other hand, flow fields generated by small stroke ratios show only a single vortex ring. The transition between these two distinct states is observed to occur at a stroke ratio of approximately 4, which, in this paper, is referred to as the 'formation number'. In all cases, the maximum circulation that a vortex ring can attain during its formation is reached at this non-dimensional time or formation number. The universality of this number was tested by generating vortex rings with different jet exit diameters and boundaries, as well as with various non-impulsive piston velocities. It is shown that the 'formation number' lies in the range of 3.6–4.5 for a broad range of flow conditions. An explanation is provided for the existence of the formation number based on the Kelvin–Benjamin variational principle for steady axis-touching vortex rings. It is shown that based on the measured impulse, circulation and energy of the observed vortex rings, the Kelvin–Benjamin principle correctly predicts the range of observed formation numbers.

1. Introduction

Vortex rings are a particularly fascinating fluid mechanical phenomenon. From starting jets to volcanic eruptions or the propulsive action of some aquatic creatures, as well as the discharge of blood from the left atrium to the left ventricular cavity in the human heart, vortex rings (or puffs) can be identified as the main flow feature. The generation, formation, and evolution of vortex rings have been the subject of numerous experimental, analytical and numerical studies. The reviews of Shariff & Leonard (1987), and Lim & Nickels (1995) describe much of the current understanding of vortex ring phenomena as well as some unresolved issues.

In the laboratory, vortex rings can be generated by the motion of a piston pushing a column of fluid of length L through an orifice or nozzle of diameter D. This results in the separation of a boundary layer at the edge of the orifice or nozzle and its subsequent spiral roll-up. The main focus of vortex ring studies in the past has been to describe the evolution of the ring's size, position, and circulation. For example, Maxworthy (1977), Didden (1979), Auerbach (1987*a*), Glezer (1988), and Glezer &

Coles (1990) studied some of the fundamental aspects of vortex ring formation as well as vortex ring trajectory and evolution. Glezer (1988) considered a few different piston velocities as a function of time known as the 'velocity program'. Didden's (1979) work has been very popular among vortex ring researchers, since it provides a clear picture of the role of internal and external boundary layers in the formation process and circulation of the vortex ring. Utilizing similarity theory, Saffman (1978) and Pullin (1979) obtained expressions for the vortex ring trajectory, circulation and its vorticity distribution. Weigand & Gharib (1997) revisited the vortex ring problem using digital particle image velocimetry (DPIV). They showed that vortex rings generated by a piston/cylinder arrangement possess a Gaussian vorticity distribution in their core region. James & Madnia (1996) present a numerical study of vortex ring formation for different generator configurations. They concluded that the total circulation and impulse in the flow field of the ring are approximately the same for nozzles with and without a vertical wall at the nozzle exit plane.

The piston/cylinder arrangement has been extensively used to address the problem of vortex ring generation. However, except for the investigations of Baird, Wairegi & Loo (1977) and Glezer (1988), all of the available experimental, analytical and numerical investigations of vortex rings use small stroke ratios (L/D). Glezer's (1988) work focused mainly on mapping the boundaries for the laminar to turbulent transition as a function of L/D, while Baird *et al.*'s work addresses the role of the impulse of the vortex ring in the formation process and presents some flow visualization observations, which we will discuss later in this paper. Therefore, to the best of our knowledge, the flow behaviour of vortex rings that can be generated with large stroke ratios (L/D) has not been examined before.

In particular, let us consider the question of the largest circulation that a vortex ring can achieve by increasing L/D, keeping the average piston velocity fixed. In general, the vorticity flux provided by the separated shear layer is the main source of vorticity for the forming vortex ring (Didden 1979). Therefore, a termination of the piston motion inhibits the flow of shear layer vorticity and thus its accumulation in the core region of the vortex ring. In this case, we should expect the circulation in the vortex formed to be approximately equal to the discharged circulation from the nozzle or orifice. In the limit of large L/D, the question arises about the existence of a limiting process which would inhibit the vortex ring from evolving (growing) indefinitely while still being fed by the vorticity emanating from the tube. In other words, for a given geometry, is there an upper limit to the maximum circulation that a vortex ring can acquire?

The purpose of this paper is to address this question. To do this, we must observe some of the global features of the vortex ring formation such as its velocity and the vorticity fields from which vortex ring circulation as a function of L/D can be obtained. We will present experimental evidence to prove the existence of such a limiting process.

2. Experimental setup

Figure 1 shows a schematic of the experimental setup. Experiments were conducted in a water tank using a constant-head tank in conjunction with a computer-controlled flow monitoring valve. Vortex rings are generated by allowing the flow from the constant-head tank to drive a piston that pushes fluid out of a sharp-edged cylindrical nozzle into the surrounding fluid. The x-axis coincides with the centreline of the vortex ring generator, and the nozzle-exit plane is located in the plane $x = 0$.

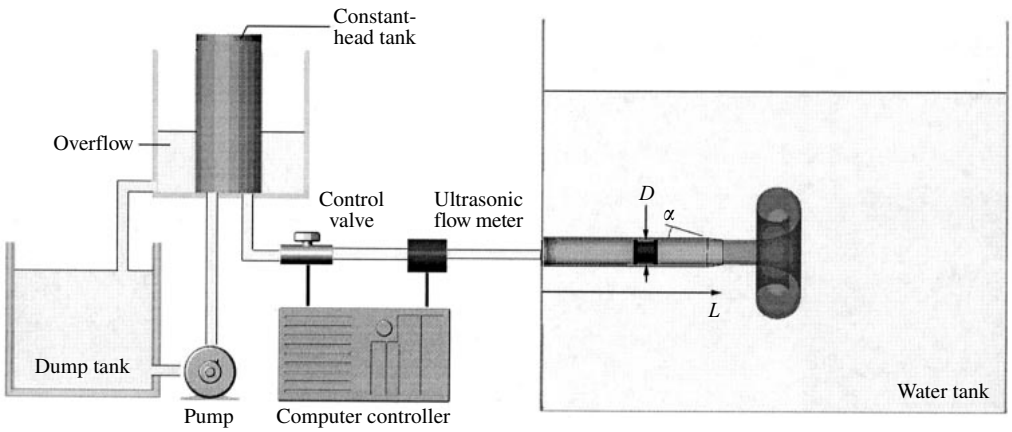

FIGURE 1. General schematic of vortex ring generator.

The main cylindrical nozzle had an inner diameter (D) of 2.54 cm. The outer contour of the cylindrical nozzle was shaped to form a wedge with a tip angle of $\alpha = 20^\circ$ and a length of 1.5 cm. In order to study the effect of the exit geometry, α was increased to 90° by simply mounting a vertical plate at the nozzle exit plane. In order to generate smaller vortex rings, a smaller nozzle with an inner diameter of 1.63 cm and an L/D of 12 was partially inserted inside the main nozzle. With this configuration, the main nozzle's piston action can be used to drive the fluid through the smaller nozzle.

A computer-controlled variable-area valve controlled the flow rate from a constant-head tank which in turn controlled the velocity program of the piston. An ultrasonic flow meter (Transonic Systems, Inc., Model T-208) was used to monitor the fluid volume displaced by the piston motion. The overall length of the cylinder limited the maximum stroke of the piston to $(L/D)_{max} = 15$ and the maximum acceleration and deceleration to $|a|_{max} \approx 250$ cm s^{-2}. Figure 2 presents typical piston velocities versus time for one case of impulsive motion and two cases of different ramp profiles. The computer control provides precise timing and synchronization of various events with a time resolution of approximately 10^{-3} s. These events include, for example, vortex ring generation and initialization of measurement processes, such as ultrasonic flow metering and DPIV.

Fluorescent dye as a fluid marker, in conjunction with a laser light sheet, was used to make the vortex ring visible. For the purposes of DPIV, the flow was seeded with neutrally buoyant silver-coated glass spheres with an average diameter of $14 \pm 5\,\mu$m and illuminated by a sheet of laser light with a thickness of approximately 0.1 cm.

The technique of DPIV (Willert & Gharib 1991), was implemented to map the flow field. DPIV measures the two-dimensional displacement-vector field of particles suspended in the flow and illuminated by a thin pulsed sheet of laser light. The present experiment used a high-speed version of DPIV that is described in detail by Weigand & Gharib (1997).

The imaging video camera was positioned normal to the measurement plane and recorded image sequences of particle fields with spatial resolution of 768×480 pixels. With a typical field of view of 11×8 cm, the spatial resolution is 0.23×0.23 cm, and the uncertainty in the velocity and vorticity measurement is $\pm 1\%$ and $\pm 3\%$, respectively.

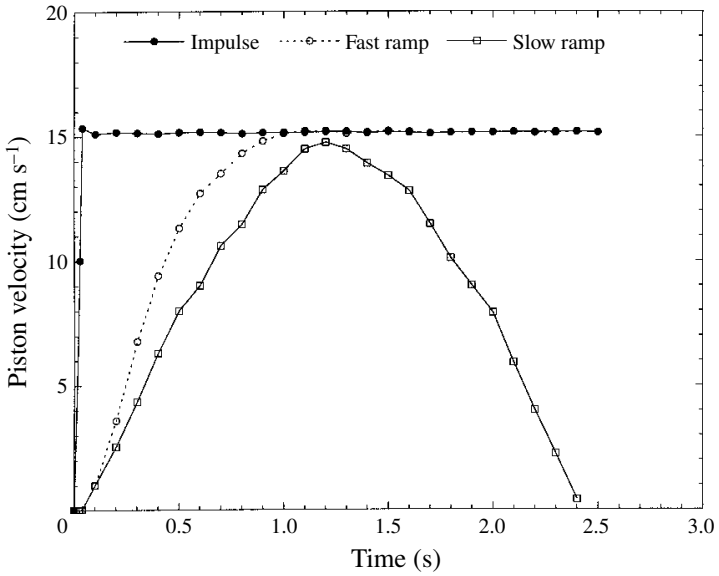

FIGURE 2. Piston velocity vs. time for three different acceleration conditions.

3. Parameters governing the vortex ring's circulation

For a given geometry, the circulation of a vortex ring (Γ) depends on the history of the piston velocity $u_p(t)$, nozzle or orifice diameter (D), kinematic viscosity (ν) and discharge time (t). The piston stroke (L) is a derived parameter related to $u_p(t)$ by $L = \int_0^t u_p(t)\mathrm{d}t$.

We introduce $\bar{U}_p$ (the running mean of the piston velocity, $\bar{U}_p = (1/t)\int_0^t u_p \mathrm{d}t$) as the suitable velocity scale. The aforementioned set of dimensional parameters can then be reduced to the non-dimensional piston velocity history $U_p(t)/\bar{U}_p$ and to two non-dimensional parameters $\Gamma/\bar{U}_p D$ and $\bar{U}_p t/D$. This non-dimensional time is equivalent to the ratio of length to diameter of the ejected fluid column (stroke ratio), i.e. $L/D = \bar{U}_p t/D$, and will be referred to as the 'formation time' in this paper.

Using the boundary layer assumption, we can show that the vorticity flux from the nozzle is approximately equal to $U_m^2/2$ where U_m is the maximum velocity within the cylinder at the exit plane. For the slug model, which assumes a uniform profile, we have $U_p^2/2 = U_m^2/2$. However, this assumption will not be valid for large stroke ratios (L/D), where the velocity profile in the pipe would show acceleration in the central region caused by the growth of the boundary layer region (Didden 1979). In this case, one needs to obtain a time history of U_m^2 and use it to normalize instantaneous circulation values. For this reason, formulas suggested by Didden, in which circulation is non-dimensionalized by $U_p D$, do not predict the circulation value for large L/D values correctly (Shariff & Leonard 1992). Glezer (1988) suggested using the kinematic viscosity (ν) to normalize circulation (Γ) as Γ/ν, which can also be considered the Reynolds number of the vortex rings. In the limits of a high Reynolds number, kinematic viscosity should not play a role in the vortex ring's formation process. In this paper, we chose to present the circulation data in its dimensional form.

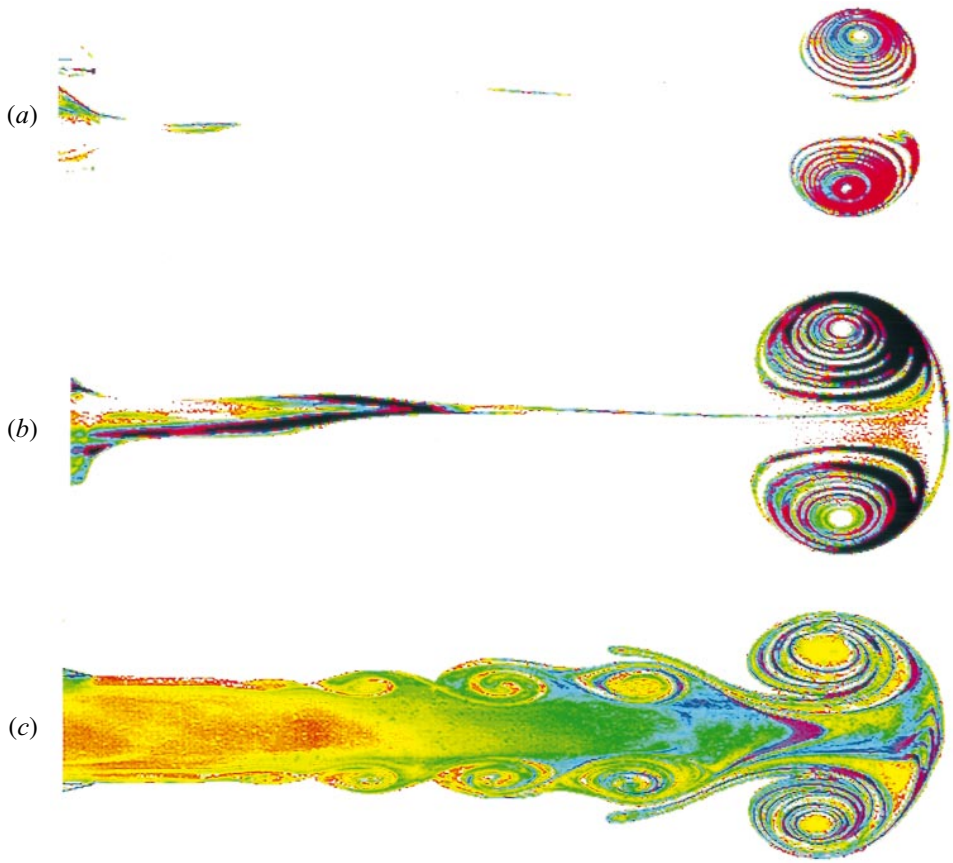

FIGURE 3. Visualization of vortex rings at $X/D \approx 9$ for (*a*) $L_m/D = 2$, $Re \approx \Gamma/\nu \approx 2800$; (*b*) $L_m/D = 3.8$, $Re \approx 6000$; and (*c*) $L_m/D = 14.5$. Picture is taken at $\bar{U}_p t/D = L/D = 8$. All three cases were generated by an impulsive piston velocity depicted in figure 2.

4. Flow visualization

Figures 3(*a*), 3(*b*) and 3(*c*) show three vortex rings generated by three different maximum stroke ratios (L_m/D). The vortex rings shown in these pictures are at an approximate axial position of $X \approx 9D$ from the nozzle exit. In figure 3(*a*), $L_m/D = 2$, while in figure 3(*b*), $L_m/D \approx 3.8$. For the case in figure 3(*c*), the piston was passing through the position $L/D \approx 8$ at the time the picture was taken. The piston motion was only stopped later at $L_m/D = 14.5$. In all cases, vortices were generated with similar impulsive piston motion to that depicted in figure 2.

One striking feature in these pictures is the existence of a trailing jet of fluid behind the leading vortex ring in figure 3(*c*) and lack of it in figures 3(*a*) and 3(*b*). It appears that in figures 3(*a*) and 3(*b*) almost all of the discharged fluid has been entrained into the vortex ring. However, for the case in figure 3(*c*), the vortex ring shows a clear separation from the active trailing jet-like region behind it. It is apparent that the formation of the vortex ring has been completed and the vorticity is no longer entrained from the shear layer region of the trailing jet. It is interesting to note that the size of the leading vortex ring in figure 3(*c*) is approximately the same as that of the vortex ring in figure 3(*b*) and is larger than that depicted in figure 3(*a*). Considering that the pictures are taken at the same downstream position of $X \approx 9D$, this variation

in the formation of the rings indicates a fundamental difference in the way that these three flows have reached their asymptotic states. A similar phenomenon can be seen in the flow visualization of Baird *et al.* (1977). But, curiously they do not report the distinction in the nature of the vortex rings formed with short and long L_m/D conditions as presented in figures 5 and 6 of their paper.

From these observations, it is natural to conjecture the existence of a limiting value for the formation time ($\bar{U}_p t/D$) or stroke ratio (L/D), for which vortex rings generated with values above this limiting value do not absorb all of the discharged fluid's mass or vorticity. The important point is to identify this limiting value $(L/D)_{lim}$ and also relate it to the vortex ring's velocity and vorticity fields. In this paper, we refer to $(L/D)_{lim}$ as the 'formation number'.

5. Velocity and vorticity fields of vortex rings

In figures 4(a, b) and 5(a, b), we present detailed measurements of velocity and vorticity fields for $L_m/D \approx 2$ and $L_m/D \approx 14.5$, respectively. These cases correspond to the flow visualizations presented in figures 3(a) and 3(c). In agreement with the visual observations, the case $L_m/D \approx 2$ does not show any noticeable level of vorticity in the trailing region after the formation of the vortex ring. On the other hand, the case $L_m/D = 14.5$ shows interesting dynamics in terms of disconnection or 'pinch-off' of both velocity and vorticity fields of vortex rings from the trailing jet. It is important to note that the vorticity in the shear layer of the trailing jet ceases to flow into the core region of the vortex ring once the pinch-off process starts. Instead, the trailing vorticity forms into a series of vortices similar to the Kelvin–Helmholtz instability.

The above observation clearly indicates the occurrence of a pinch-off process which causes termination of the vorticity flow into the ring and further increase of the circulation level in the ring. From the vorticity contours, one can obtain the total discharged circulation by integrating the vorticity contained within the lowest detectable contours for either positive or negative senses. In our observations, this contour level was determined to be at $1\,\mathrm{s}^{-1}$. Also, in the absence of the trailing jet, the total circulation level was not very sensitive to the choice of the level, as long as this was chosen to visually contain the desired vorticity region. However, for the cases where a trailing jet-like region appears, the vortex ring circulation can only be measured when a clear separation between vorticity contours of the vortex from those of the trailing region exists. In this case, circulation of the vortex was determined at a larger X/D position where the pinch-off process was clearly complete.

6. Circulation of the vortex ring as a function of the maximum stroke ratio (L_m/D) and formation time ($\bar{U}_p t/D$)

We performed two sets of experiments in order to identify the transition between vortex rings with and without trailing jet flow.

In the first set of experiments, vortex rings were generated by limiting the maximum stroke ratio (L_m/D) to set values in the range of 0.5 to 6.7. Also, for mechanical reasons, the maximum impulse velocity was limited to 7.5 cm s^{-1}. For each case, the maximum circulation of the vortex formed (of either positive or negative sense) was measured by integrating the vorticity within an iso-vorticity contour (of a given sense) of $1\,\mathrm{s}^{-1}$. The results for circulation vs. maximum stroke ratio (L_m/D) are shown in figure 6.

It is interesting to note that for a given set of flow parameters, the maximum

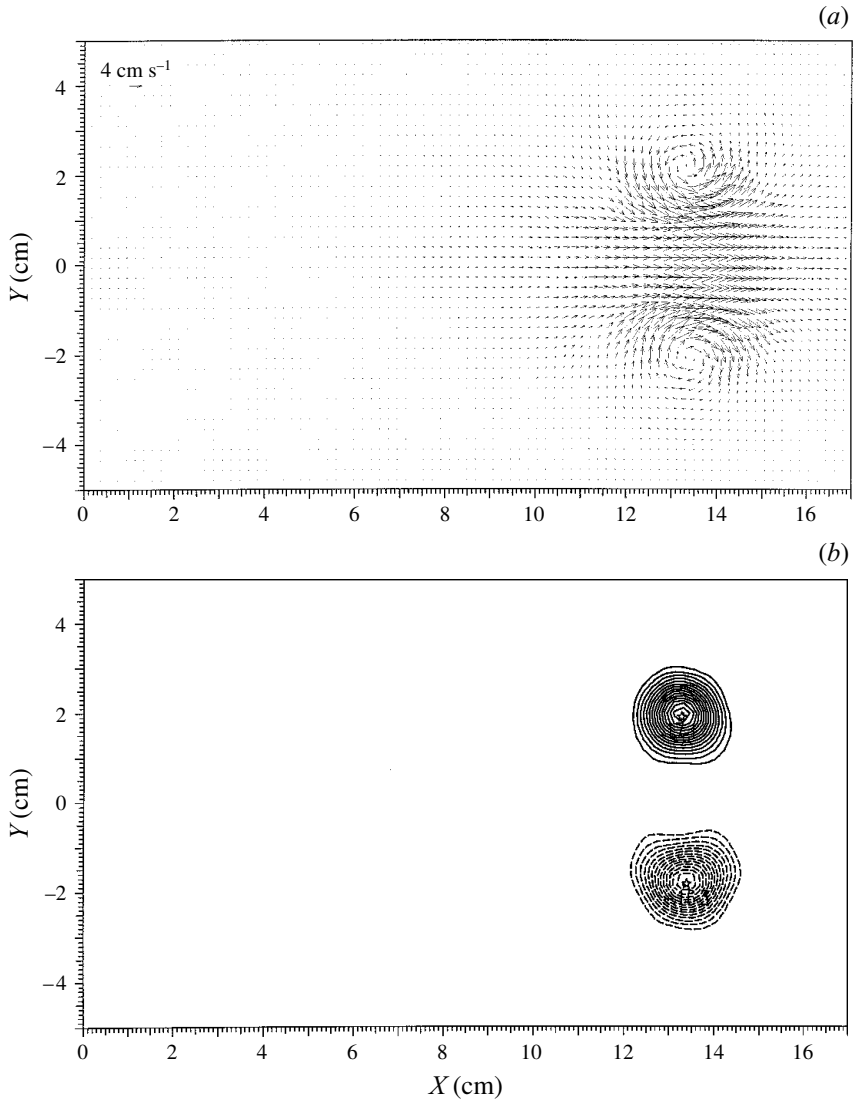

FIGURE 4. (*a*) Velocity vector and (*b*) vorticity fields of a vortex ring with $L_m/D \approx 2$.

circulation that the vortex ring can attain is reached with L_m/D in the range of 4 to 5. Therefore, we should expect the limiting value $(L/D)_{lim}$ or 'formation number' to reside in this range.

In the second set of experiments, we measured the circulation emanating from the cylinder and the vortex ring as a function of the formation time† or $\bar{U}_p t/D = L/D$. In these experiments, the piston was impulsively started with $U_p = 7.5$ cm s^{-1} and was stopped when $L/D \approx 8$ (i.e. for this case $L_m/D \approx 8$). The main difference between the second and the first set of experiments is that in the first set the formation process was not interrupted by the stopping of the piston at the end of each run. For this

† Non-dimensional time or $\bar{U}_p t/D$ for each case is equivalent to the stroke ratio (L/D). For the points after the piston stops, we used the last value of $\bar{U}_p$ in calculating the non-dimensional time.

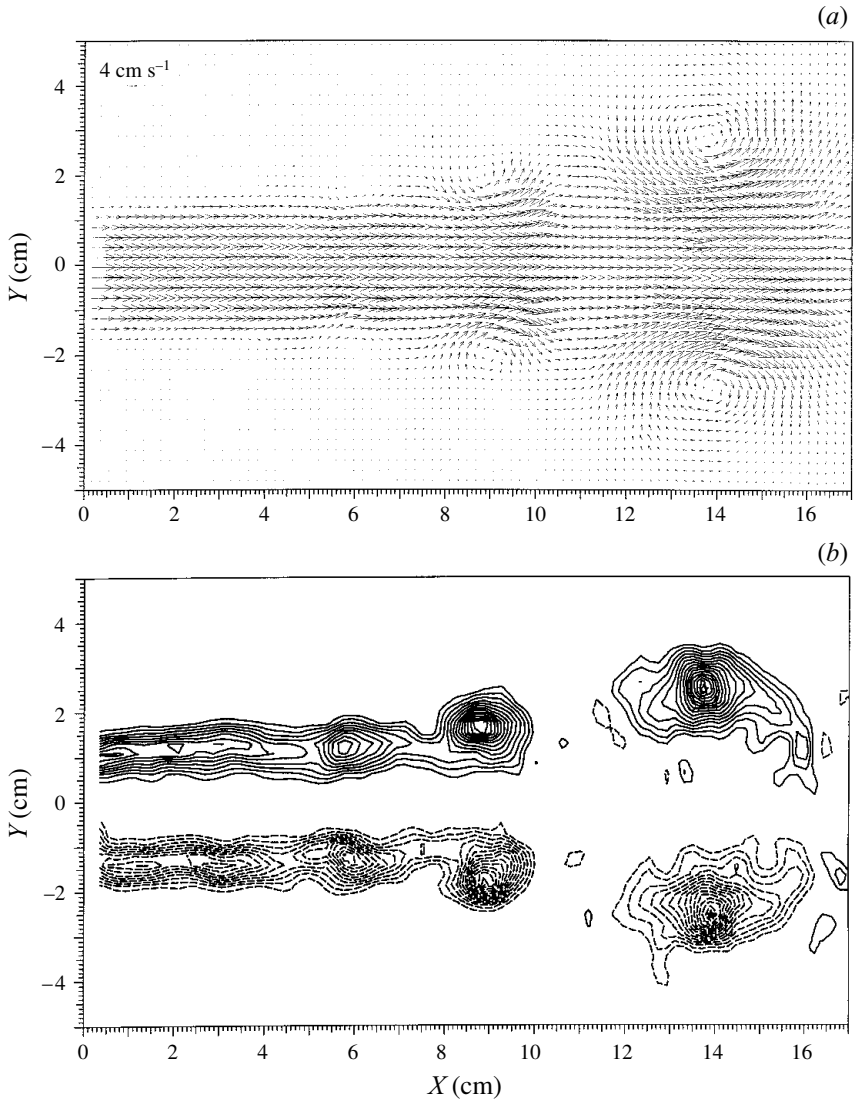

FIGURE 5. (*a*) Velocity vector and (*b*) voriticity field of a vortex ring with $L_m/D \approx 14.5$ corresponding to case (*c*) in figure 3.

case, the total circulation and the maximum circulation of the vortex ring after its formation was measured at each time step.

In figure 7, the maximum circulation of a vortex ring is shown by open circles and the total circulation by solid circles. As is expected, after $L/D \approx 8$ (when the piston stops) the total circulation remains at a constant level of $50\,\mathrm{cm^2\,s^{-1}}$. The vortex ring formed shows a circulation level of $28 \pm 1\,\mathrm{cm^2\,s^{-1}}$ corresponding to a Reynolds number (Γ/ν, where Γ is the circulation of the pinched-off vortex ring) of approximately 2800. As is shown by a straight line on the plot, at a formation time of approximately 4, the vortex generator has produced a circulation level of $28\,\mathrm{cm^2\,s^{-1}}$, which is equivalent to that of the vortex ring formed.

From these observations, we can infer that only the vorticity that has emanated

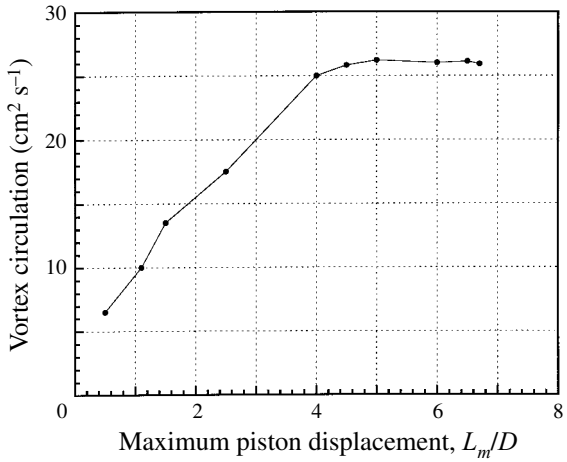

FIGURE 6. Vortex ring circulation as a function of L_m/D with $D \approx 2.54$ cm.

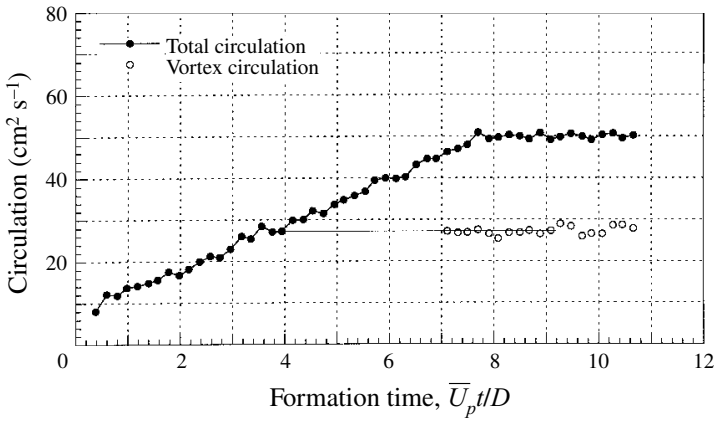

FIGURE 7. Vortex ring circulation as a function of formation time ($\bar{U}_p t/D$) for the case $L_m/D \approx 8$, $D = 2.54$ cm and $Re = \Gamma/\nu \approx 2800$ for pinched-off vortex ring.

from the cylinder exit plane, up to $\bar{U}_p t/D$ or L/D of approximately 4, will accumulate in the vortex ring; and, should the piston be forced to stop at $L/D \approx 4$, the resulting vortex ring will leave no trailing jet. In other words, the maximum circulation that the vortex ring could attain is equivalent to the total circulation discharged from the nozzle up to the threshold formation time or formation number of 4. The pinch-off process is not a sudden event and its completion might take up to two formation time units to complete. Since selection of a proper level of vorticity contour for the purpose of separating the vortex ring from its trailing shear layer can be subjective, the nature of the pinch-off process could not be resolved with enough confidence. Therefore, most of our circulation measurements for the vortex ring were obtained at large X/D values where the pinch-off process has already been completed.

7. Formation number for other flow conditions

In the next series of experiments, we reduced the diameter of the vortex generator to $D = 1.63$ cm. This provides vortex rings with somewhat different diameters. We

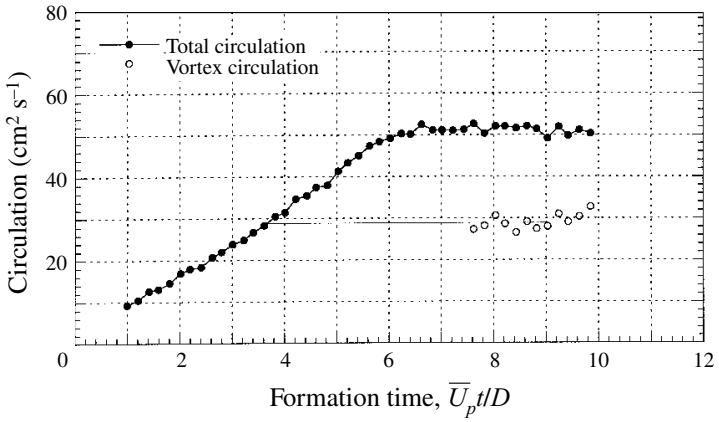

FIGURE 8. Vortex ring circulation as a function of formation time ($\bar{U}_p t/D$) for the case $L_m/D \approx 6$, $D = 1.63$ and $Re = \Gamma/\nu \approx 2800$ for the pinched-off vortex ring.

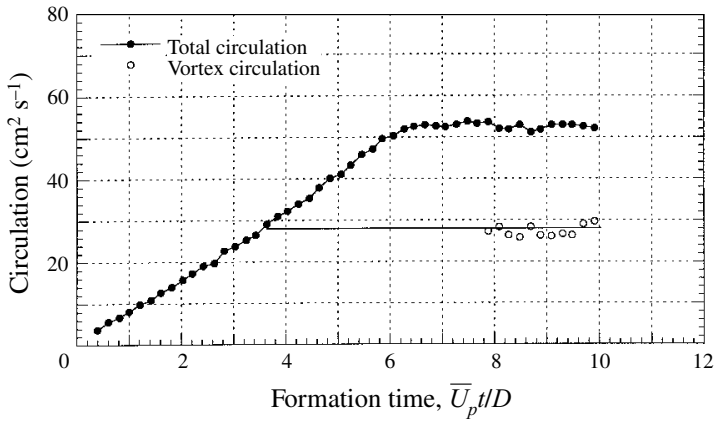

FIGURE 9. Vortex ring circulation as a function of formation time ($\bar{U}_p t/D$) for the case of $L_m/D \approx 6$, $D = 1.63$ cm with the wall ($\alpha = 90°$). $Re = \Gamma/\nu \approx 2800$ for the pinched-off vortex ring.

also adjusted the maximum impulsive piston velocity in order to keep the Reynolds number in the same range as in the case with a diameter of 2.54 cm. It can be seen in figure 8 that with a formation number of about 3.8 ± 0.2, the total discharged circulation reaches the maximum circulation of the vortex ring. This value of the formation number is very close to that obtained for the large-diameter vortex ring case presented in figure 7. Next, a solid wall was installed at the plane of the nozzle exit. Therefore, the angle α (shown in figure 1), was increased to 90°. Figure 9 shows that the maximum level of circulation for the rings decreased slightly which resulted in a lower value of the formation number ($\bar{U}_p t/D \approx 3.6$). This reduction can be attributed to the opposite-sign vorticity generated in the secondary boundary layer on the outside wall and its entrainment by the vortex ring. However, it is interesting that the drastic nature of the change in the boundary condition has not resulted in any major shift in the formation number.

In the next set of experiments, we raised the maximum impulsive piston velocity to 15 cm s^{-1} (figure 2). This provides us with a vortex ring at a Reynolds number

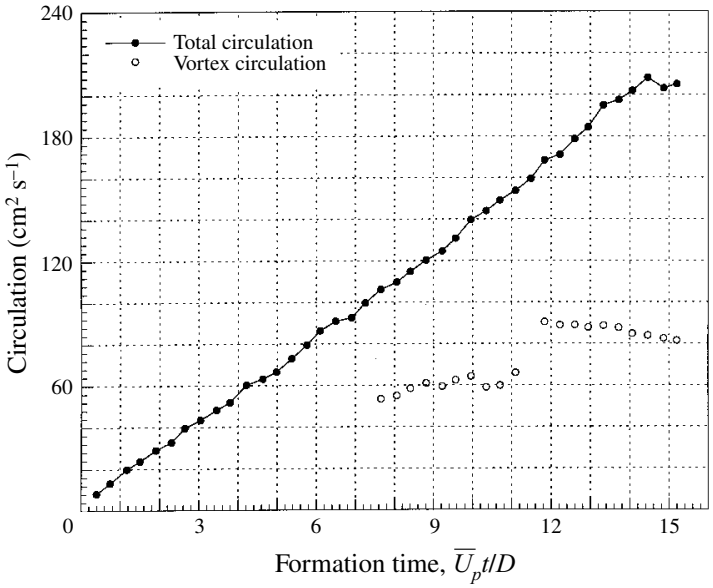

FIGURE 10. Vortex ring circulation as a function of formation time ($\bar{U}_p t/D$) for the case of impulsive piston motion, $L_m/D \approx 14.5$, $D = 2.54$ cm and $Re = \Gamma/\nu \approx 6000$ for the pinched-off vortex ring.

of 6000, which is twice that in the previous case. This case also corresponds to the flow visualization images in figure 3(*c*) and velocity and vorticity field series in figure 5. Figure 10 presents the total circulation and vortex ring circulation vs. formation time for this case. A formation number of approximately 4.2 can be associated with the time that the maximum circulation of the ring is reached. But, in this case, the leading vortex of the trailing jet had eventually caught up with the pinched-off vortex and, therefore, the circulation level was increased with a step-like behaviour. However, long-time ($\bar{U}_p t/D > 13$) observation of vortex rings suggests that the vortex started to shed this excess vorticity and, therefore, reduced its circulation at large X/D values. Figure 11 presents the streamwise position of the pinched-off vortex ring as a function of $\bar{U}_p t/D = L/D$ for this case. This plot indicates that the forming vortex ring reaches a steady translating velocity (represented by a constant slope) for $\bar{U}_p t/D > 4$. This behaviour was common for all the pinched-off vortex rings in our study. For $L/D > 10$, because of the increased circulation due to the leap-frogging, a non-constant slope was observed. This behaviour is not shown in figure 11.

Next, we studied vortex rings generated by two different start-up ramps of 16 cm s^{-2} and 22 cm s^{-2} (figure 2). In the first case, the piston was decelerated back to zero velocity; in the second case, the piston continued to move steadily after the initial acceleration phase. For the slower ramp with acceleration 16 cm s^{-2}, the formation number is approximately 4.5 (figure 12). For the faster ramp with acceleration of 22 cm s^{-2}, where the piston continued to move steadily after $t = 1$ s, the formation number is 4.2 (figure 13). This case also shows the step-like increase of circulation due to the catching up by the leading vortex of the trailing jet with the vortex formed similar to the case depicted in figure 10.

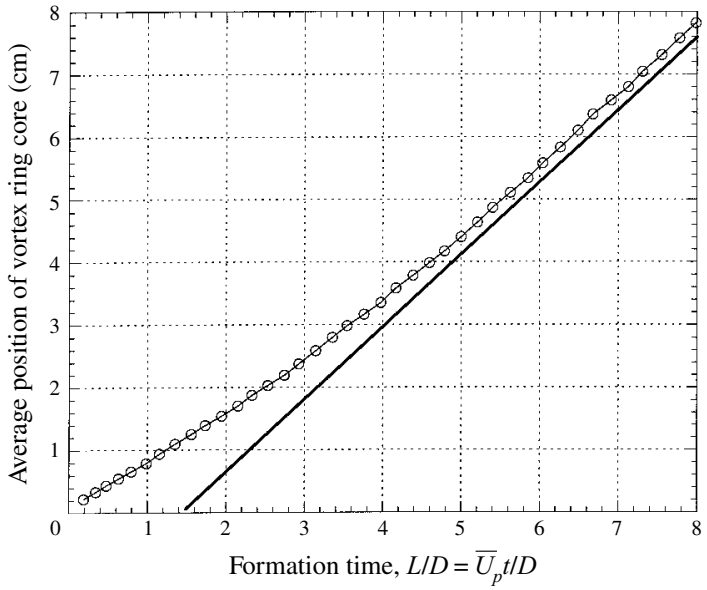

FIGURE 11. Average position of vortex ring core as a function of formation time for the case in figure 10. The line is superimposed for comparison with the line position for the experimental curve.

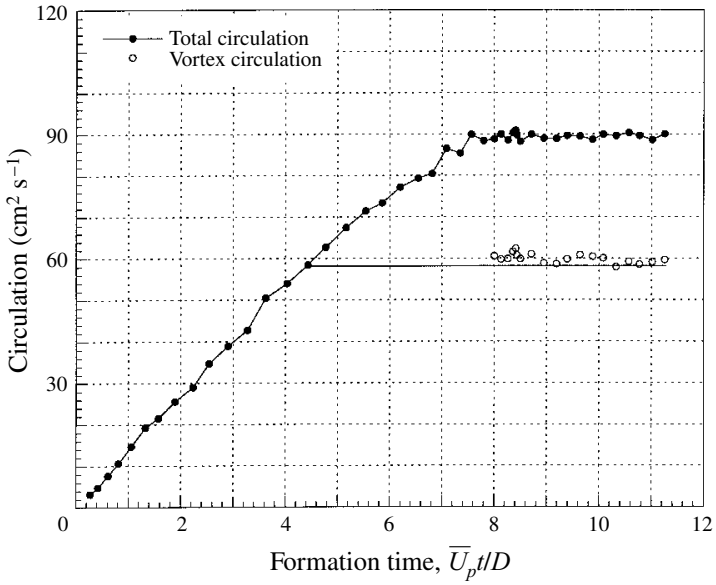

FIGURE 12. Vortex ring circulation as a function of $\bar{U}_p t/D$ for slow-ramp case (16 cm s^{-2}) $L_m/D \approx 12.5$, $D = 2.54$ cm, $Re = \Gamma/\nu \approx 6000$ for the pinched-off vortex ring.

8. The analytical model

The results reported in the previous sections are a small sample of many runs (in excess of 30) with different velocity and acceleration conditions. Without exception, the observed formation number, when the maximum value of circulation in a vortex ring is reached, falls in the range of 3.6 to 4.5. In general, the presence of boundaries

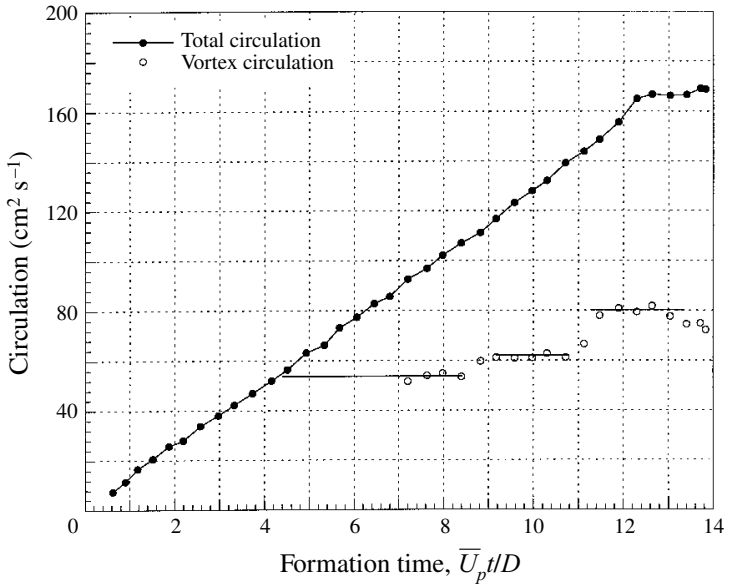

FIGURE 13. Vortex ring circulation as a function of $\bar{U}_p t/D$ for fast-ramp case (22 cm s^{-2}) $L_m/D \approx 8$, $D = 2.54$ cm, $Re = \Gamma/\nu \approx 6000$ for the pinched-off vortex ring.

shifts the formation number toward lower values, while non-impulsive and higher Reynolds number flows shifts it towards high values. This section attempts to predict this seemingly robust number.

The model is based on the hypothesis that the limiting stroke, $(L/D)_{lim}$, occurs when the apparatus is no longer able to deliver energy at a rate compatible with the requirement that a steadily translating vortex ring have maximum energy with respect to impulse-preserving iso-vortical perturbations.† This suggests that we consider a non-dimensional energy

$$\alpha \equiv \frac{E}{I^{1/2}\Gamma^{3/2}}, \tag{1}$$

where E and I are the kinetic energy and impulse, respectively, with density set to unity. At any instant during the formation, $\Delta\alpha(t) = \alpha_{steady}(t) - \alpha_{piston}(t) > 0$ measures the departure from a single steady ring. Here $\alpha_{steady}(t)$ is the value of α for that steady vortex ring which is accessible from the vorticity field at time t via an iso-vortical impulse-preserving rearrangement.

We will see that $\alpha_{piston}(t)$ decreases inexorably as $\approx (\pi/2)^{1/2}(L(t)/D)^{-1}$ for a variety of piston programs. On the other hand, for each family of steady vortex rings, we expect α to diminish to a limiting value, α_{lim}, as the core thickens. Thus $\alpha_{piston}(t) < \alpha_{lim}$ after some critical value of $L(t)/D$ and the departure from a steady ring will increase. This critical value defines the limiting stroke.

Some cautionary remarks are in order.

(i) A quasi-steady formation process has been assumed in which $\alpha_{piston}(t)$ remains

† *Iso-vortical* means that the circulation of each fluid element is preserved. Kelvin (1880, §§4 and 18) states the variational principle without proof as being obvious to him. In particular, he states that in the axisymmetric case the energy must be an absolute maximum. Benjamin (1976), in apparent ignorance of Kelvin's result, states the same result. He proves that the first variation is zero but no proof is provided that the second variation is negative.

close to $\alpha_{steady}(t)$ for as long as $\alpha_{piston}(t) > \alpha_{lim}$. A sequence of short piston pulses, for instance, is not allowed.

(ii) The existence of a limiting α for every family of steady vortex rings (defined by a given vorticity versus streamfunction relation $\omega/r = f(\psi)$) is an unproven generalization based on the Norbury–Fraenkel (Norbury 1973) family.

(iii) α_{lim} is an unknown parameter that depends on the peakiness of the vorticity profile which in turn depends on piston history and Reynolds number (Pullin 1979; Saffman 1978). To emphasize this we shall write $\alpha_{lim} = \alpha_{lim}[U_p; Re_p]$. For the Norbury–Fraenkel family, $\omega/r = \text{const}$, Hill's vortex is the limiting member, and $\alpha_{lim} = 0.16$. The discussion in Fraenkel (1972, pp. 127–128), valid for thin cores, suggests that α_{lim} is larger than 0.16 for families with peaked vorticity. For the experimental axis-touching rings in figures 10 and 12 we obtained $\alpha_{lim} = 0.33 \pm 0.01$ without a clear trend for the 'impulsive' or 'slow-ramp' piston velocity programs. The Reynolds numbers for the two cases are 2800 and 6000. This value of α was obtained from DPIV measurements using the following relations:

$$E = \pi \int \omega\psi \, \mathrm{d}x\mathrm{d}r, \qquad I = \pi \int \omega r^2 \, \mathrm{d}x\mathrm{d}r, \qquad \Gamma = \int \omega \, \mathrm{d}x\mathrm{d}r. \tag{2}$$

What happens after $\alpha(t) < \alpha_{lim}$? Pozrikidis (1986) found that when Hill's vortex is perturbed it either returns to a smaller Hill's vortex by shedding a tail or evolves to a (presumably unsteady) ring with a hole by entraining irrotational fluid. The pinch-off observed experimentally is analogous to tail shedding. Both occur because vorticity in the outer regions of the core finds itself in the region where fluid particles are being swept past the ring instead of revolving around it. Thus we expect that if $\alpha(t) < \alpha_{lim}$, rings will either shed vorticity or not accept any new vorticity in order to maintain $\alpha = \alpha_{lim}$ within a single ring. This is consistent with the experiments. Figure 14 shows the measured vorticity along a radial line that cuts through the two cores. Early on, the vorticity is confined to Gaussian-like cores. However at the final frame, which corresponds to the instant when $(L/D)_{lim}$ occurs, the ring has become axis touching, i.e. ω/r extends to the symmetry axis. Subsequently the ring pinches off and translates steadily (figure 11). Even more striking is the case presented in figure 10 where a trailing ring temporarily merged with the leading ring. In this configuration the value of α dropped to 0.25. Eventually, however (approximately (3 to 4) $\overline{U}_p t/D$ later), the vortex ring shed circulation and α returned to $\alpha_{lim} = 0.33$.

Next we evaluate α_{piston}, the α delivered by the apparatus. The circulation is obtained by integrating the vorticity flux from a thin boundary layer with edge velocity equal to the piston speed. The limitations of this assumption are reviewed in Shariff & Leonard (1992). We get

$$\Gamma(t) = \tfrac{1}{2} t \overline{U_p^2}, \tag{3}$$

where henceforth a bar will denote a time average over the interval $[0, t]$. To calculate impulse and energy, the velocity across the entire exit is assumed to be the piston speed and exit pressure is assumed to equal ambient pressure. The latter is also the condition invoked for oscillations in open-ended tubes (e.g. Wijngaarden 1968). The reasoning is that if the shear layer is thin compared to the length scale of axial variations (so we have essentially a rectilinear flow) the radial pressure gradient is negligible. This assumption deserves future study since initially the flow is like a potential source which creates a pressure difference from the ambient.

The impulse is the space-time integral of imposed forces which create the vortex ring

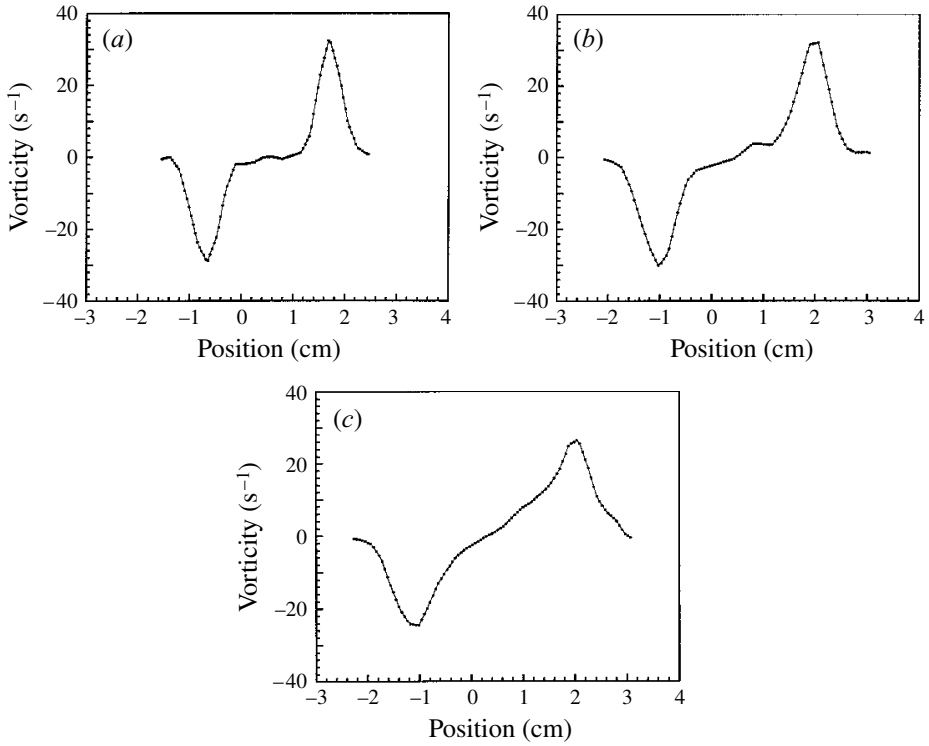

FIGURE 14. Vorticity distribution along a line connecting two cores of a vortex ring depicted in figure 5. (*a*) $X/D = 0.59$, (*b*) $X/D = 1.77$, (*c*) $X/D = 3.35$.

in an unbounded medium. Cantwell (1986) has shown that the pressure disturbance at infinity counteracts a third of the imposed forces. Hence the fluid momentum ends up being 2/3 of the impulse applied. For the present case, performing a balance of momentum in the region of fluid external to the pipe (assuming exit pressure is the ambient pressure) we reason that the force at infinity counteracts the momentum flux from the pipe so that the momentum in the region is 2/3 of that emitted from the pipe. Hence we conclude that the ring impulse is equal to the total momentum flux from the exit:

$$I \approx \pi R^2 t \overline{U_p^2}. \tag{4}$$

The work done by the pressure force at infinity is zero and so for the kinetic energy we get

$$E \approx \tfrac{1}{2}\pi R^2 t \overline{U_p^3}. \tag{5}$$

Other procedures for estimating these global quantities are also possible, including the one due to Saffman (1975).

Substituting (3), (4) and (5) into (1) gives

$$\alpha_{piston}(t) = \left(\frac{\pi}{2}\right)^{1/2} \left(\frac{L}{D}\right)^{-1} M[U_p; t] \quad \text{where} \quad M[U_p; t] \equiv \frac{(\overline{U_p^3})\overline{U_p}}{(\overline{U_p^2})^2}. \tag{6}$$

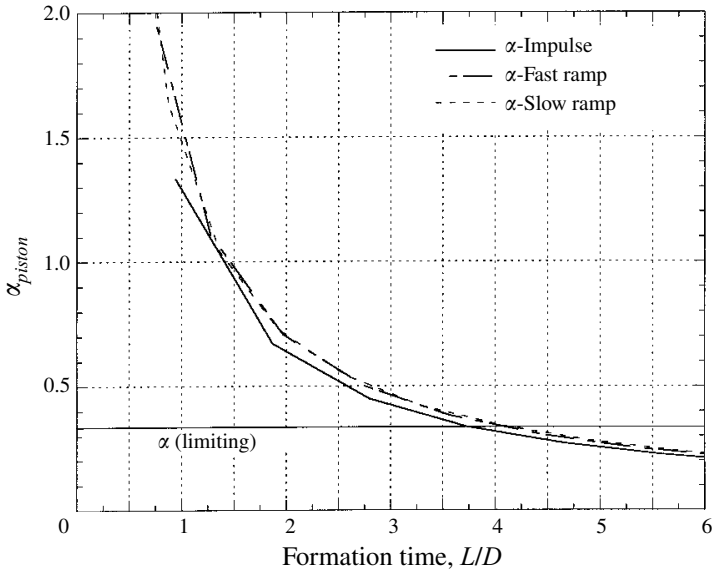

FIGURE 15. Variation of parameter α with formation time ($\bar{U}_p t/D = L/D$) for the piston velocities in figure 2.

One can also write more compactly

$$M[U_p; t] \equiv \frac{\widetilde{U_p^2}}{(\widetilde{U_p})^2}, \tag{7}$$

where $\tilde{}$ denotes an average with respect to $L(\tau)/D$ for $\tau \in [0, t]$.

The hypothesis is that a single steady ring is no longer possible when

$$\alpha_{piston}[U_p; t] < \alpha_{lim}[U_p, Re_p] \quad \text{or} \quad \frac{L}{D} > \left(\frac{\pi}{2}\right)^{1/2} \frac{M[U_p; t]}{\alpha_{lim}[U_p; Re_p]}. \tag{8}$$

Figure 15 plots α_{piston} for the three piston velocities shown in figure 2. The three curves are nearly identical when plotted against L/D and the condition (8) with $\alpha_{lim} = 0.33$ gives the limiting stroke as $(L/D)_{lim} \approx 4$. This agrees remarkably well with the experiments. Note the slightly increased $(L/D)_{lim}$ for the fast and slow ramps which is also in accord with our experiments. This is a consequence of the fact that $M \geqslant 1$ with equality holding for uniform piston speed (which follows from the Cauchy–Schwartz–Buniakowsky inequality). Figure 17 shows α_{piston} calculated for some hypothetical piston profiles shown in figure 16. There is little variation among the different α_{piston} curves and if we take $\alpha_{lim} = 0.33$ the range of $(L/D)_{lim}$ is 4 to 5.

The insensitivity of $(L/D)_{lim}$ is due to the insensitivity of M to U_p as well as due to the experimentally observed insensitivity of $\alpha_{lim}[U_p; Re_p]$ in the range of the parameter space explored in the experiments. We would like to suggest the possibility that some other piston velocities could give a quite different $(L/D)_{lim}$. To investigate the range of variability of $(L/D)_{lim}$ consider a time interval $[0, T]$ where T corresponds to the instant (unknown *a priori*) of $(L/D)_{lim}$. For convenience introduce $\xi = t/T$ and a scaled piston speed, $V(\xi)$, whose maximum value is unity in the time interval. Then increases in $M[V_p(\xi); \xi = 1]$ correspond directly to increases in $(L/D)_{lim}$ with α_{lim}

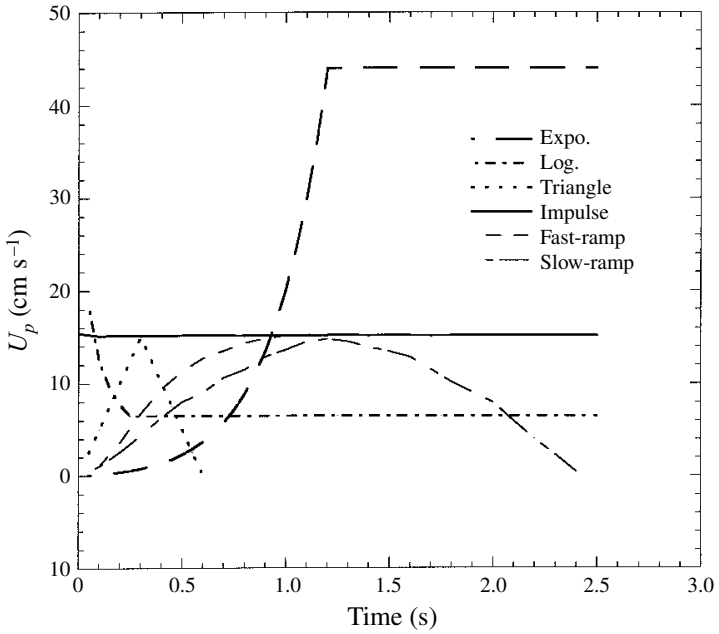

FIGURE 16. Piston velocity vs. time for hypothetical piston velocities. As a reference, the experimental velocities from figure 2 have been superimposed.

fixed. For $V(\xi) = \xi^m$, the form considered in self-similar roll-up theories (e.g. Pullin 1979), one gets

$$M[\xi] = \frac{(2m+1)^2}{(3m+1)(m+1)}.$$

This varies from unity at $m = 0$ to only $4/3$ at $m = \infty$ which is also the value of M for exponential $V(\xi)$. Pullin's equation (13) shows that flatter vorticity distributions are produced with larger m which should diminish α_{lim} and help the increase in $(L/D)_{lim}$. Next, consider functions for which M is not a constant and investigate the variability of $M[V_p(\xi);\ \xi = 1]$. Since this quantity involves only integrals of powers of $V_p(\xi)$ over a fixed interval, it is independent of rearrangements of $V_p(\xi)$. For instance if $V_p(\xi)$ peaks at $\xi = 1$, a flipped version that peaks $\xi = 0$ would produce the same $M[\xi = 1]$. Consider

$$V_p(\xi) = \frac{\exp(\xi^2/\sigma^2) - 1}{\exp(1/\sigma^2) - 1},$$

which starts at zero and rises to a peak over a region of width $\sim \sigma$. For this case $M[\xi = 1]$ has a maximum of 1.38 for $\sigma \approx 0.41$, which is still not significantly different from unity. The quantity $M[V_p(\xi);\ \xi = 1]$ can be made arbitrarily large. Consider a unit pulse of width δ rising above a background of height ϵ:

$$V_p(\xi) = \begin{cases} \epsilon, & 0 < \xi < (1-\delta) \\ 1, & (1-\delta) \leqslant \xi < 1. \end{cases}$$

The location of the unit pulse is at the right-hand end of the interval but could be placed anywhere without affecting the result. In the limit $\epsilon \to 0$ and $\delta \to 0$ as ϵ^2, $M[V_p(\xi);\ \xi = 1]$ becomes arbitrarily large. Such a piston velocity has infinite acceleration and in reality one would place a constraint on the maximum acceleration.

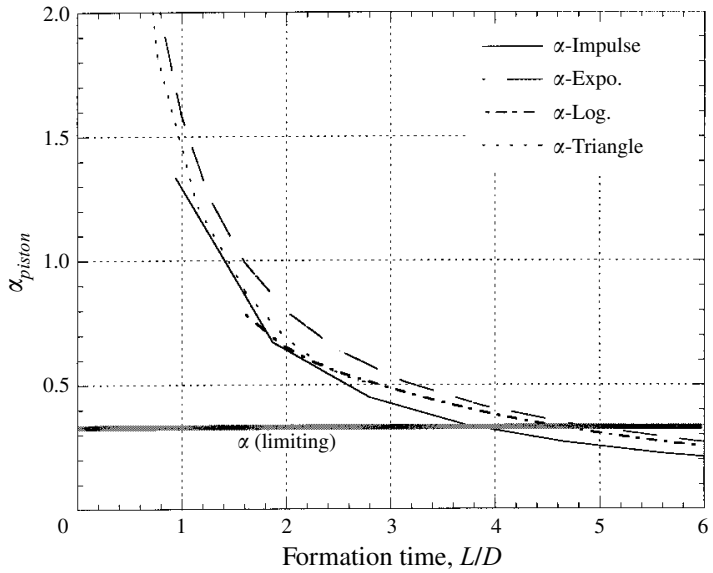

FIGURE 17. Variation of parameter α with formation time ($\bar{U}_p t/D = L/D$) for the hypothetical piston velocity program in figure 16.

Numerical maximization of the functional $M[V_p(\xi);\ \xi = 1]$ subject to the constraint $|V_p'(\xi)| < a_{max}$ was performed. The end conditions $V_p(0) = 0$ and $V_p(1) = 1$ were applied. It revealed the optimum to be of the form

$$V_p(\xi) = \begin{cases} a_{max}\,\xi, & 0 \leqslant \xi < V_0/a_{max} \\ V_0, & V_0/a_{max} \leqslant \xi < \xi_1 \\ V_0 + a_{max}(\xi - \xi_1), & \xi_1 \leqslant \xi \leqslant 1. \end{cases}$$

For a given a_{max} the value of V_0 which maximizes $M[V_p(\xi);\ \xi = 1]$ may be determined. For instance with $a_{max} = 5$, $M[V_p(\xi), 1]$ attains a maximum value of ≈ 1.65 for $V_0 \approx 0.12$. All of these examples suggest that to raise $M[V_p(\xi), 1]$ significantly above unity requires a long stretch of small piston speed with a short pulse of high speed. If the low-speed portion precedes the high-speed portion, the vorticity distribution is flatter than for uniform U_p thus reducing α_{lim} and increasing $(L/D)_{lim}$ even further. More precise statements than this about the effect of piston history on α_{lim} would be useful. In practice, one has to place some constraints on the long stretch of the small piston speed, preventing it from dropping the jet's Reynolds number too far to where viscous dissipation might become dominant and prevent the roll-up process.

Professor M. Rosenfeld (private communication) of Tel-Aviv University recently performed numerical simulations of vortex ring formation and found that the exit velocity profile has a significant influence on formation number $(\overline{U}_b t/D)_{lim}$. Here $U_b(t)$ is the bulk velocity (volumetric flow rate/area). In particular, for a parabolic profile the formation number is reduced to unity from the present value of about 4 for a uniform profile. Working out the fluxes of impulse, etc. for the parabolic profile, one finds that the parabolic equation (6) is modifed by the replacements: $U_p \rightarrow U_b$ and $L \rightarrow \overline{U}_b t$. Moreover, a factor of $\sqrt{3}/8 \approx 0.22$ is introduced which nicely accounts for the observed reduction provided the vorticity peakiness parameter, α_{lim}, has the same value as here (0.33).

9. Concluding remarks

The formation of vortices in nature or industrial processes in the absence of a density gradient usually involves boundary layer separation and ejection of a column of fluid from a confined volume. In this respect, the piston cylinder setup is a reasonable representative of the formation of vortices in nature or in the laboratory. In this paper, we have demonstrated that a time scale with a narrow range of values characterizes the formation of vortex rings in the piston/cylinder setup. This time scale (referred to as the formation number) is the time beyond which larger rings are not possible. We demonstrated that this observed narrow range for the formation number is a direct manifestation of the variational principle proposed by Kelvin and Benjamin for steady axis-touching rings.

Several interesting cases were observed but were not pursued further in this study. For example, for some impulsive and non-impulsive piston motions, it was possible to increase the circulation of a vortex ring after its formation through entrainment of the leading vortex of the trailing jet by the vortex ring. Therefore, it was possible to increase the level of circulation in a vortex ring even after initial disconnection from the trailing jet. However, we observed that the vortex ring reduced its circulation by shedding the excess vorticity into its wake. Such shedding of vorticity had previously been observed by Maxworthy (1977) and Weigand & Gharib (1995). But whether this shedding is the only mechanism of reduction of the circulation of the vortex or other mechanisms, such as viscous annihilation, might be present is not clear. In another situation, a ring was overtaken by a faster trailing jet. This usually resulted in the destruction of the ring and was not considered a normal condition in the formation process.

The mere existence of the formation number is intriguing since it hints at the possibility that nature uses this time scale for some evolutionary incentives such as optimum ejection of blood from the left atrium to the heart's left ventricle or locomotion process where ejection of vortices might have been utilized for the purposes of propulsion.

This work has been conducted through a grant from ONR (URI N00014-91-J-1610) and a grant from NIH (PHS-1-7R01-HL43287-03). We would like to thank Professor C. Pozrikidis and S.-H. Lam for numerous discussions regarding Hill's vortices and the vortex formation process. We are also indebted to Professor P. Saffman for pointing out that the pedigree of the energy maximization principle extends to Kelvin. Professors H. Johari and M. Rosenfeld, and Drs M. Hammache, F. Noca, and D. Dabiri; and R. Henderson and D. Jeon have, in various capacities, contributed to the progress and completion of this work.

REFERENCES

Auerbach, D. 1987 Experiments on the trajectory and circulation of the starting vortex. *J. Fluid Mech.* **183**, 185–198.

Baird, M., Wairegi, H. I. & Loo, H. J. 1977 Velocity and momentum of vortex rings in relation to formation parameters. *Can. J. Chem. Engng* **55**, 19–26.

Batchelor, G. K. 1967 *An Introduction to Fluid Dynamics*. Cambridge University Press.

Benjamin, T. B. 1976 The alliance of practical and analytical insights into the non-linear problems of fluid mechanics. In *Applications of Methods of Functional Analysis to Problems in Mechanics*, (ed. P. Germain & B. Nayroles). Lecture Notes in Mathematics, vol. 503, pp. 8–28. Springer.

Cantwell, B. J. 1986 Viscous starting jets. *J. Fluid Mech.* **173**, 159–189.

Didden, N. 1979 On the formation of vortex rings rolling-up and production of circulation. *Z. Angew. Math. Phys.* **30**, 101–116.

Fraenkel, L. E. 1972 Examples of steady vortex rings of small cross-section in an ideal fluid. *J. Fluid Mech.* **51**, 119–135.

Glezer, A. 1988 The formation of vortex rings. *Phys. Fluids* **31**, 3532–3542.

Glezer, A. & Coles, D. 1990 An experimental study of a turbulent vortex ring. *J. Fluid Mech.* 221, 243–283.

Hill, M. J. M. 1894 On a spherical vortex. *Phil. Trans. R. Soc. Lond.* A**185**, 213–245.

James, S. & Madnia, K. 1996 Direct numerical simulation of a laminar vortex ring. *Phys. Fluids* **8**, 2400–2414.

Kelvin, Lord 1880 Vortex statics. *Phil. Mag.* **10**, 97–109.

Lim, T. T. & Nickels, T. B. 1995 Vortex rings. In *Vortices in Fluid Flows* (ed. by S. I. Green). Kluwer.

Maxworthy, T. 1977 Some experimental studies of vortex rings. *J. Fluid Mech.* **81**, 465–495.

Norbury, J. 1973 A family of steady vortex rings. *J. Fluid Mech.* **57**, 417–443.

Pozrikidis, C. 1986 The non-linear instability of Hill's vortex. *J. Fluid Mech.* **168**, 337–67.

Pullin, D. 1979 Vortex ring formation at tube and orifice opening. *Phys. Fluids* **22**, 401–403.

Saffman, P. G. 1975 On the formation of vortex rings. *Stud. Appl. Maths* **54**, 261–268.

Saffman, P. 1978 The number of waves on unstable vortex rings. *J. Fluid Mech.* **84**, 625–639.

Saffman, P. G. 1992 *Vortex Dynamics.* Cambridge University Press.

Shariff, K. & Leonard, A. 1992 Vortex Rings. *Ann. Rev. Fluid Mech.* **24**, 235–279.

Weigand, A. & Gharib, M. 1995 Turbulent vortex ring/free surface interaction. *Trans. ASME J. Fluids Engng* **117**, 374–381.

Weigand, A. & Gharib, M. 1997 On the evolution of laminar vortex rings. *Exps. Fluids* **22**, 447–457.

Wijngaarden, L. van 1968 On the oscillations near and at resonance in open tubes. *J. Engng Maths* **2**, 225–240.

Willert, C. & Gharib, M. 1991 Digital particle image velocimetry. *Exps. Fluids* **10**, 181–193.